JOURNAL OF THE ROYAL SOCIETY Interface

J. R. Soc. Interface (2012) **9**, 1733–1744
doi:10.1098/rsif.2011.0825
Published online 8 February 2012

High-resolution microrheology in the pericellular matrix of prostate cancer cells

Nadja Nijenhuis[1], Daisuke Mizuno[2], Jos A. E. Spaan[1,*] and Christoph F. Schmidt[3,*]

[1]*Department of Biomedical Engineering and Physics, Academic Medical Center, University of Amsterdam, PO Box 22660, 1100 DD Amsterdam, The Netherlands*
[2]*Organization for the Promotion of Advanced Research, Kyushu University, Fukuoka, Japan*
[3]*Drittes Physikalisches Institut, Fakultät für Physik, Georg-August-Universität, Friedrich-Hund-Platz 1, 37077 Göttingen, Germany*

Many cells express a membrane-coupled external mechanical layer, the pericellular matrix (PCM), which often contains long-chain polymers. Its role and properties are not entirely known, but its functions are believed to include physical protection, mechanosensing, chemical signalling or lubrication. The viscoelastic response of the PCM, with polysaccharides as the main structural components, is therefore crucial for the understanding of its function. We have here applied microrheology, based on optically trapped micrometre-sized colloids, to the PCM of cultured PC3 prostate cancer cells. This technology allowed us to measure the extremely soft response of the PCM, with approximately 1 μm height resolution. Exogenously added aggrecan, a hyaluronan-binding proteoglycan, caused a remarkable increase in thickness of the viscoelastic layer and also triggered filopodia-like protrusions. The viscoelastic response of the PCM, however, did not change significantly.

Keywords: hyaluronan; optical tweezers; prostate cancer cells; elastic shear modulus

1. INTRODUCTION

In many tissues, cells are embedded in extracellular matrices (ECMs) of proteins, fibres and polysaccharides. The cell-associated pericellular matrix (PCM) mediates between the cell and the ECM and plays important mechanical roles in various cellular processes including proliferation, migration and mechanosensing [1–4]. The PCM is rapidly formed during mitotic cell rounding and is observed mostly at the trailing edge of migrating cells, facilitating their detachment [1,4]. A particular PCM, the endothelial glycocalyx (EG), is expressed by vascular endothelial cells, forming the interface between the flowing blood and the underlying cell layer, acting as a protective barrier and mechanotransducer of shear stress [5–7]. The molecular composition of the PCM depends on the cell type. Chondrocytes, for example, incorporate collagen in their PCM [2], while this protein is absent in the EG [8]. All PCMs, however, contain the glycosaminoglycan hyaluronan (HA) as the largest molecular weight component and as the mechanical backbone. Prior studies suggest that HA plays a crucial role in the structural and mechanical integrity of the PCM. Degradation of HA causes the PCM to collapse. Replacing native high molecular weight HA by HA oligosaccharides results in inhibition of cell migration and proliferation [4]. Motility and the invasive nature of osteosarcoma cells are abolished by the same treatment [9], which suggests an involvement of the PCM in cancer cell metastasis. Endothelial cells lose their ability to respond to fluid flow when HA is enzymatically removed [7]. On the other hand, it is possible to artificially enhance the PCM. Addition of both HA and a HA-binding proteoglycan of the hyalectin family [10,11], such as aggrecan or versican, to various cells expressing HA-binding receptors was shown to stimulate an extended PCM [1,12].

The mechanical environment of cells has recently been shown to strongly influence cell properties and behaviour, such as stiffness [13], proliferation and motility [14,15], as well as differentiation [16,17]. Elucidating the mechanics of the PCM is therefore of key importance for the understanding of its physical and physiological functions. Atomic force microscopy (AFM) and micropipette aspiration have been used to quantify the mechanical properties of the PCM of chondrocytes from human tissue cartilage [18,19]. This type of PCM in tissue was found to be relatively stiff with a Young's modulus of 40–100 kPa [19] when probed with micropipette aspiration or AFM. Such high-elastic moduli for healthy cartilage, and a decreased pericellular stiffness (approx. 20 kPa) for osteoarthritic cartilage [18]

*Authors for correspondence (j.a.spaan@amc.uva.nl; cfs@physik3.gwdg.de).

Electronic supplementary material is available at http://dx.doi.org/10.1098/rsif.2011.0825 or via http://rsif.royalsocietypublishing.org.

Received 25 November 2011
Accepted 13 January 2012

are in accordance with the load-bearing role of articular cartilage. For invasive metastatic cancer cells that need to be motile and malleable, the PCM is expected to be much softer. It has been difficult to measure the elasticity of such soft PCMs because a technique like AFM requires forces of at least tens of piconewton [20], too much for very soft materials. Here, we introduce passive microrheology, a technique previously used to mechanically characterize polymer solutions, to probe the soft PCM of metastatic prostate epithelial cancer cells (PC3 cell line). With this method, we can measure the local viscoelasticity of materials by observing the spontaneous thermal fluctuations of optically trapped (sub-)micron colloidal particles [20]. Thus, instead of having to apply large external perturbations to the PCM, we employed here only minimally invasive microrheology. By using an optical trap, we could manipulate the position of the probe particle in the PCM and thus measure its stiffness at different heights above the membrane. Determining a shear elastic modulus implicitly assumes that the material can be treated as homogeneous, at least on the scale of the probe particles. This assumption can clearly break down in and around cells that typically have a highly complex and inhomogeneous structure on all length scales. As a coarse-grained approximation, the approach is nevertheless expected to provide useful estimates of material properties on micrometre scales, larger than the molecular scale and smaller than the scale of gross cellular features.

We probed the immediate periphery of PC3 cells up to about 10 μm radial distance from the outer cell membrane, and quantitatively resolved the local viscoelasticity of the PCM with about 1 μm resolution. PC3 cells are HA-producing cells. The presence of high levels of HA and versican in the peritumoral stroma has been shown to be correlated to the metastatic spread of clinical prostate cancer [21,22]. Riccardelli *et al.* [1] showed an increase in motility for PC3 cells that incorporate HA and versican in their PCM, and suggest that *in situ* PC3 cells recruit stromal versican to remodel their PCM and enhance their motility.

We used aggrecan (a commercially available chondroitin sulphate proteoglycan similar to, and from the same family as, versican) as a substitute to examine the effect of such a proteoglycan on the mechanical properties of the PCM. We found that upon exogenous addition of aggrecan, the PCMs on these HA-producing cells were enhanced and filopodia-like protrusions were seen to project from the cell surface. Both the extended viscoelastic PCM and the protrusions induced by aggrecan disappeared after the addition of hyaluronidase (HAase), which confirmed the critical importance of HA for the structure of the PCM.

2. MATERIAL AND METHODS

2.1. Sample preparation

The culture medium DMEM, as well as antibiotic–antimycotic, non-essential amino acid solution, trypsin and inactivated foetal bovine serum (FBS) were obtained from Invitrogen (Carlsbad, CA, USA). Phosphate-buffered saline (PBS, pH 7.4) was purchased from Fresenius Kabi (Bad Homburg, Germany) and silica spheres (0.8 μm diameter, 50 mg l^{-1}) from G. Kisker GbR (Steinfurt, Germany). Aggrecan and HAase (bovine testis, fraction IV-S) were obtained from Sigma–Aldrich (St Louis, MO, USA). Sodium hyaluronate in powder form, with a weight-average molecular weight (M_w) of 1844 kDa was obtained from LifeCore Biomedical (Chaska, MN, USA). Fibronectin was a kind gift from the Sanquin Research Foundation (Amsterdam, The Netherlands). PC3 cells (human prostate adenocarcinoma cell line) were grown at 37°C in 5 per cent CO_2 in cell culture flasks coated with 10 mg ml^{-1} fibronectin. Cells were cultured in D-MEM supplemented with 10 per cent FBS, 1 per cent non-essential amino acid solution and 1 per cent antibiotic–antimycotic solution. For each microrheology measurement, cells were trypsinized, taken from a culture flask and seeded on a glass coverslip, located in a re-usable glass chamber (see electronic supplementary material, figure S1). The bottom of the chamber was made of a microscope slide. The spacers at the four sides were made of glass, with a height of 0.39 mm. The spacers were glued to the slide glass with silicon resin, forming an inner volume of $22 \times 14 \times 0.39$ mm^3. After seeding, cells were incubated for 90 min before the culture medium was replaced by either new culture medium without any extra additives, or with culture medium containing aggrecan (1 mg ml^{-1}) with or without HAase (40 units ml^{-1}). After 90 min, 0.8 μm silica beads were added and the chamber was sealed by a coverslip placed on top of the spacers. Measurements were done at room temperature (21.8°C) within an hour after the sample was taken out of the incubator.

As a control, we constructed an *in vitro* model system. For this experiment, HA was dissolved in PBS and mixed with aggrecan (1 mg ml^{-1}) to a final HA concentration of 2.5 mg ml^{-1}.

2.2. Immunofluorescence confocal imaging

To verify whether the aggrecan-induced protrusions of the PC3 cells, which we observed with differential interference contrast (DIC) microscopy in the microrheology experiments, contained actin, we performed confocal fluorescence microscopy with PC3 cells incubated with 1 mg ml^{-1} aggrecan. The PC3 cells were seeded on glass coverslips and incubated for 90 min with normal culture medium, using a protocol identical to that used in the microrheology measurements. After a further 90 min of incubation with aggrecan (1 mg ml^{-1}), the cells were fixed with paraformaldehyde (4%). After 10 min, the paraformaldehyde was removed and the cells were washed with PBS (two times). The cells were then stained with Alexa Fluor 555 phalloidin (5 U ml^{-1}, Molecular Probes) for 60 min. After a final wash with PBS, the cells were mounted on a microscope slide and sealed. We used 50 per cent glycerol in PBS as mounting medium.

Fluorescent images of actin-containing filopodia-like protrusions were obtained with a confocal microscope (Leica TCS SP2). Z-scans were made with a step size of 120 nm. Data were analysed and projected onto cross sections vertical to the glass surface using WCIF ImageJ software.

2.3. Microrheology

The microrheology measurements were performed using a custom-built microscope set-up including an optical trap, essentially implementing earlier designs [23]. The set-up was built around, and attached to an upright microscope equipped with a DIC imaging option (Olympus BX51WI). Its water immersion objective (UPlanApo, 60×, NA = 1.2, Olympus) was used to focus an 830 nm laser beam (diode laser, cw, 140 mW, 1Q1C140 G5, Laser 2000) in the sample chamber. The thermal motion of a trapped 0.8 μm silica bead, illuminated by the laser inside the chamber, was detected with a quadrant photodiode (diameter = 10 mm; SPOT-9DMI, UDT Sensors, Hawthorne, CA, USA) using back-focal plane interferometry [24]. For optimal trapping, the laser was expanded (three times) by a beam expander (LINOS Photonics, Germany). The laser power was controlled by a combination of a half-wave plate and a polarizer. A 1 : 1 telescope system was used for fine-positioning and steering of the beam focus. To detect the position of the trapped bead, the outgoing laser light interfering with the scattered light from the bead was collected by a condenser lens (NA = 0.8, WI-UCP, Olympus), and projected onto a quadrant photodiode (diameter = 10 mm, SPOT-9DMI, UDT Sensors), which was positioned in a plane conjugate to the back-focal plane of the condenser lens [24]. The four output signals of the quadrant photodiode were processed with analogue amplifiers to produce signals coding for the *x*- and *y*- positions of the trapped bead in two directions parallel to the sample plane. These voltages were recorded using an A/D data acquisition board (PCI-4451, National Instruments, Austin, TX, USA) operated with LabView software (National Instruments). Data were taken with a sampling rate of 195 kHz (approx. 2×10^6 data points). The precise z-positioning of the trapped bead was achieved by mounting the objective lens on a piezo-driven, nano-focusing device (P-720, Physik Instrumente) that was computer controlled. The microscope was operated in high-contrast DIC mode.

Measurements were started about 10 μm above the cell surface. The probe bead was then brought closer to the cell in initial steps of 1 μm and ending with steps of 0.5 μm for the last 2 μm to the cell surface. When the focus of the laser beam started to cross into the cell, the bead was displaced from the centre of the trap, leading to a readily detected loss of quadrant photodiode signal. A distance of 0.5 μm above this point was set as the origin of the height coordinate ($h = 0$ μm). The height h thus corresponded to the distance between the bead surface and the cell membrane. After each approach to the cell surface through the PCM, we brought the probe bead up again and took another reference measurement at $h = 25$ μm.

2.4. Shear modulus determination

The method used to derive the shear modulus of the surrounding material from the displacement fluctuation spectrum of the probe particles embedded in the material is given in detail elsewhere [20,23,25,26]. In short, the fluctuation–dissipation theorem relates the calculated power-spectral density, $S(\omega)$, of the position fluctuations of the probe particles to the imaginary part of the complex response function $\alpha(\omega) = \alpha'(\omega) + i\alpha''(\omega)$ as $\alpha''(\omega) = (1/4k_BT)\omega S(\omega)$, with k_B the Boltzmann constant, and T the temperature of the solution. If $\alpha''(\omega)$ is measured over a wide frequency range, a Kramers–Kronig integral can be used to obtain $\alpha'(\omega) = (2/\pi)\int_0^\infty dt \cos(\omega t) \int_0^\infty d\xi \alpha''(\xi) \sin(\xi t)$. In the case of a spherical particle, as in our experiments, a generalized Stokes–Einstein equation can be used to derive the complex shear modulus: $G(\omega) = 1/(6\pi a \alpha(\omega))$, with a the bead radius, and G' and G'' the real (elastic) and imaginary (viscous) part of the shear modulus, respectively. Before this final step is taken, however, the complex response function needs to be corrected for the contribution of the optical trap to the measured response: $\alpha_{cor} = \alpha/(1 - k_t\alpha)$, where k_t is the trap stiffness and α the uncorrected response [27]. In principle, a strong laser trap limits fluctuations at low frequencies. Our laser power, however, was limited to less than 70 mW in the sample. Therefore, this effect was not a problem. At a laser power of the order of 100 mW, we expect an increase in local temperature of about 0.5 K, which creates a negligible error in comparison with other sources of errors [28]. For a purely viscous medium of viscosity η, the Stokes relation is recovered by using $G(\omega) = -i\omega\eta$.

2.5. Correction for surface effects (Faxen's law)

In earlier studies, we used oil-immersion objective lenses [27,29–31] for which spherical aberration leads to a height dependence of calibration factors and trap stiffness [32]. Here, we used a water-immersion lens instead, for which calibration factors and trap stiffness are independent of height [32]. There is, however, hydrodynamic interaction between the particle and the glass surface that becomes relevant at distances from the surface comparable with the particle size. This interaction results in an increased viscous drag ζ for purely viscous liquids, which is described by Faxen's law [33]. For general viscoelastic materials, such as the PCM, the same description applies to a frequency-dependent complex drag $\zeta^* = 6\pi i\omega G a$. In our scanning microrheometry measurements, this effect was first probed for by measuring the apparent viscous modulus as a function of height above the glass surface in a place where no cells were present (taken as an average over eight height scans; electronic supplementary material, figure S2). Correction factors for each height point were then obtained as shown in the electronic supplementary material, figure S2 by dividing the apparent G'' by the value measured at a distance of 25 μm where calibration recordings were taken. We then calculated estimates for the shear moduli of the PCM by dividing the apparent G' and G'' values measured above the cells by the height-dependent correction factors.

3. RESULTS AND DISCUSSION

3.1. Microrheology of the pericellular matrix

We first confirmed, using a particle exclusion assay, that PC3 cells were surrounded by a several micrometre-thick

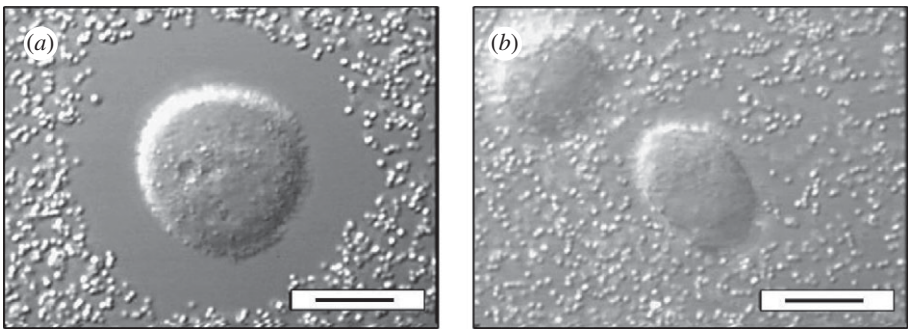

Figure 1. Pericellular matrix (PCM) of PC3 cells, incubated with aggrecan in the culture medium, indirectly visualized using a particle exclusion assay with 0.8 μm silica particles. (*a*) The exclusion zone indicates a 5–10 μm thick PCM. (*b*) The exclusion zone disappears upon co-incubation with HAase. Scale bars (*a*,*b*), 10 μm.

PCM when incubated with aggrecan (figure 1*a* and electronic supplementary material, figure S3). Particles, identical to the silica probe particles that were subsequently used in the microrheology experiments, could not enter the immediate periphery of the PC3 cells by diffusion. The exclusion of the probe particles from the cell periphery indicates the presence of a dense layer of extracellular material. Cells co-incubated with HAase, in contrast, lost this impenetrable layer as can be seen in figure 1*b*. Microrheology experiments with laser-trapped 0.8 μm silica beads embedded in the PCM were then carried out at different distances from the cell surface in the presence of aggrecan in the culture medium (see §2). The same general method with the same type of probe particles was used in our prior studies characterizing HA solutions [31] and composites made of HA and aggrecan [34].

Probe particles had to be inserted into the PCM using the optical trap because diffusional access was hindered. Probe articles could be moved smoothly into the PCM without observing any stress build-up and rupture events as one would expect if major structural damage would accompany the insertion of the beads (see electronic supplementary material, movie S1, for a recorded bead movement by the laser trap through the PCM). Typical results for the shear elastic (figure 2*a*) and viscous (figure 2*b*) modulus as a function of frequency are shown at different heights above the cell surface.

For a complete quantitative characterization of the PCM, it will be essential to have a detailed knowledge of all molecular components and their potentially inhomogeneous distribution in the PCM. This information is not available yet for the PCM of PC3 cells or any other cell type. One can, however, compare our data with results obtained from well-controlled model systems. In earlier studies, we reconstituted *in vitro* model systems composed of the major structural components of the PCM: HA, aggrecan and the glycosaminoglycans (GAGs) heparan sulphate (HS) and chondroitin sulphate (CS) [31,34]. HA (with physiological molecular weight of approx. 2000 kDa) was the component that dominated the viscoelastic response of the model PCMs [34], while aggrecan slightly increased the viscoelasticity and other GAGs, such as CS and HS did not have a strong effect on the PCM rheology unless their concentration was higher than 10 mg ml^{-1}, which we think is irrelevant for the PCM of the PC3 cells.

In earlier work [31], we characterized *in vitro* HA networks and showed that the complex shear modulus of non-cross-linked HA networks with physiological MW can be approximately modelled as a sum of three contributions (equation (3.1)), two owing to the polymer network and one from direct solvent friction: the first term describes long-time relaxation by reptation and an intermediate plateau region (when $\beta = 1$), the second term describes high-frequency power-law behaviour of the network, and the third term describes viscous friction of the bead in the solvent:

$$G(\omega) = \frac{\mathrm{i}\omega\eta_0}{1 + (\mathrm{i}\omega\tau)^{\beta}} + B(\mathrm{i}\omega)^{\gamma} + \mathrm{i}\omega\eta, \qquad (3.1)$$

with η_0 being the effective low-frequency network viscosity, τ the repational relaxation time, η the viscosity of water and B a material-dependent prefactor. In our case of a membrane-attached PCM, we do not expect long-time relaxation to be possible. In a system exhibiting more than a single collective characteristic frequency at intermediate frequencies, for example owing to polymer length polydispersity, the exponent β can be smaller than 1, leading to power-law behaviour of $G(\omega)$ with an exponent $1-\beta$. We found empirically that our data can be well fit with a single exponent at the lower frequencies, so that we use the approximation:

$$G(\omega) \approx B(\mathrm{i}\omega)^{\gamma} + \mathrm{i}\omega\eta, \qquad (3.2)$$

At high frequencies, the overall response eventually approaches the solvent response because the frequency dependence of the polymer-network contribution is sub-linear ($\gamma < 1$) [23]. The prefactor B is expected to be approximately proportional to the concentration of the polymer constituents, but does not strongly depend on the type of polymers or their molecular weights. At frequencies accessible to our microrheology technique (<100 kHz), a solvent-dominated mechanical response was observed in the model systems only for polymer concentrations less than approximately 2.5 mg ml^{-1} [31]. In our PC3 cell experiments, the response was close to solvent-dominated at all heights above the cells, implying that the concentration of the large molecular-weight PCM constituents is not more than approximately 2.5 mg ml^{-1}. Comparing the magnitude of the measured elastic modulus with the model studies as in an earlier study [33] shows that

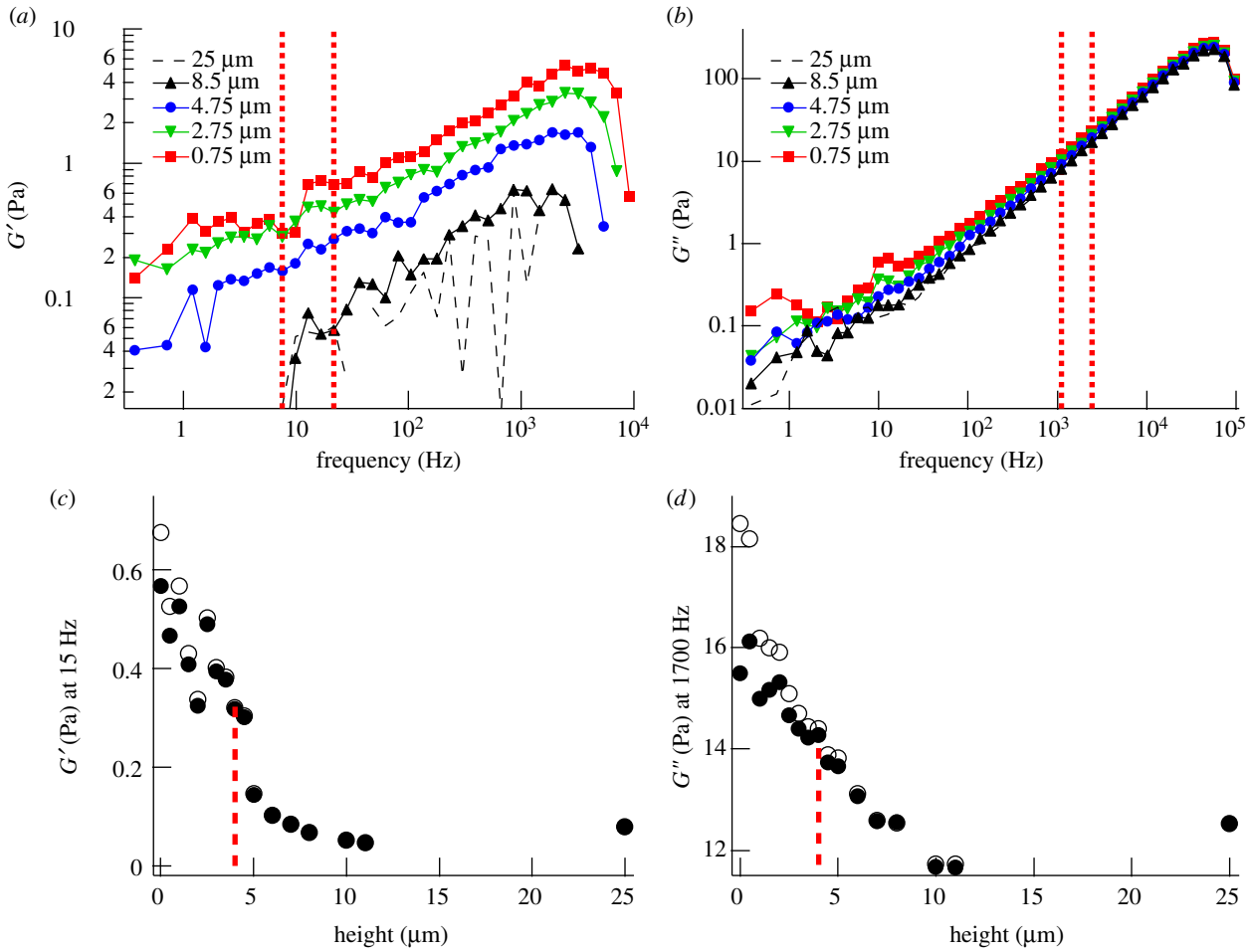

Figure 2. Mechanical properties of the PCM of a PC3 cell incubated with aggrecan, but without visible protrusions, probed by microrheology with a 0.8 µm silica bead. (*a*) Elastic modulus (G') and (*b*) viscous modulus (G'') at different heights above the PC3 cell surface. Height is measured between the cell surface and the bead surface. (*c*) Radial map of G' (around 15 Hz) and (*d*) G'' (around 1700 Hz) through the pericellular region. Open symbols are uncorrected data, filled symbols are data corrected for the influence of the nearby surface (Faxen). Data between vertical dashed lines (7–22 Hz) in (*a*) and between vertical dashed lines (1100–2200 Hz) in (*b*) were averaged for each height, and results are shown in (*c*) and (*d*), respectively. Vertical dotted lines in (*c*) and (*d*) indicate the characteristic thickness λ of the PCM. Open circles, uncorrected; closed circles, Faxen-corrected.

the modulus found for the PCM is comparable with the modulus for a 1 mg ml^{-1} HA solution. A plateau-like elastic modulus G' at low frequencies is an indication for the mechanical reinforcement of a polymer network either by cross-linking or entanglement of the polymers. In the PCM of the PC3 cells, we did not find a plateau for G' (figure 2*a*) [27,29–31], but, instead, continuous power-law behaviour: $G' \propto Re[B(\mathrm{i}\omega)^{\gamma}]$ ($\gamma \sim 0.5$ for the aggrecan-extended PCM, and $\gamma \sim 0.3$ for the unextended PCM) over a wide frequency range (figure 3). We had found in the model system that the power-law slope γ of the low-frequency relaxation is highly dependent on the concentration of HA and reduces to approximately 0.5 at concentrations less than approximately 2.5 mg ml^{-1}, which is consistent with our experimental observations in the PCM of PC3 cells. Given that the HA concentration is probably below approximately 2.5 mg ml^{-1}, we assume that HA in the PCM is semi-dilute, not strongly entangled. This also explains the finding that the elasticity of the PCM is highly dependent on the distance from the cell surface, which—in that case—provides the main fixed anchor point.

In figure 3, we compare the frequency dependence of the viscoelastic modulus of the model PCM (condition: HA 2.5 mg ml^{-1}, aggrecan 1 mg ml^{-1}) and the cellular PCM (height = 0 µm). They show qualitative similarity in the intermediate- and high-frequency regions. The solid curve is the fit of the model PCM as shown by equation (3.2) ($\gamma = 0.49$). The main difference between the mechanical response of the model PCM system and the cellular PCM is that the moduli of the model HA decrease more steeply towards low frequencies ($\omega < 1/\tau$), probably owing to reptational disentanglement, which is not possible for the HA in the PCM that is bound to the cell membrane.

To visualize the variation of low- and intermediate-frequency response with distance from the cell surface, we plotted the elastic modulus G' around 15 Hz (taken as an average between 7 and 22 Hz) as a function of height (figure 2*c*), and the viscous modulus G'' around 1700 Hz (taken as an average between 1100 and 2200 Hz), as a function of height (figure 2*d*). Choosing, in the latter case, a relatively high frequency, beyond most physiological dynamics, is useful because the response at such a high frequency should

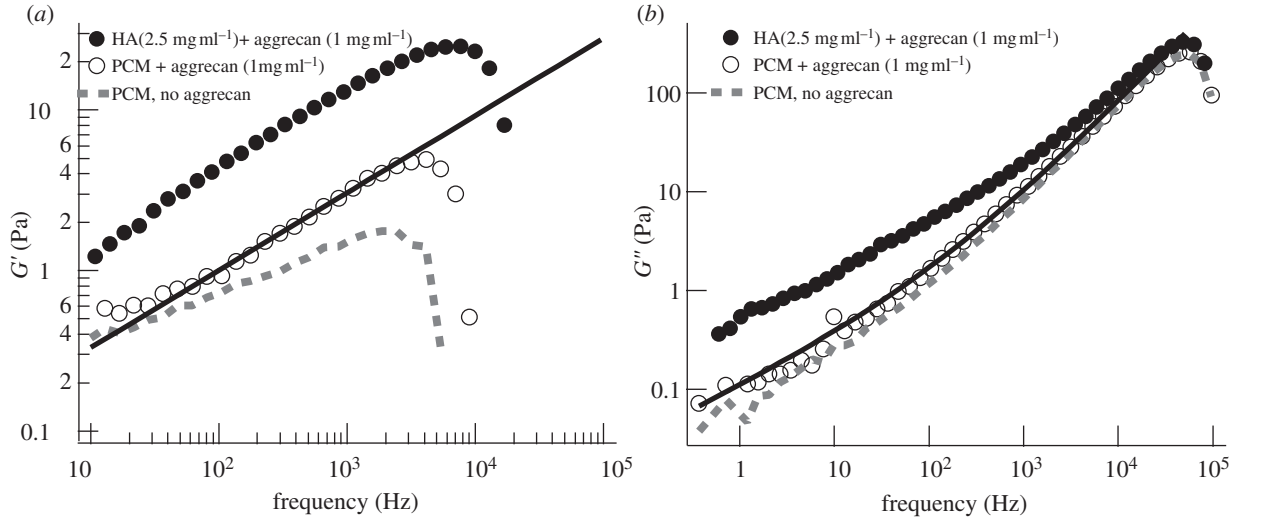

Figure 3. Comparison of the mechanical properties of the PCM as expressed by PC3 cells in the presence (or absence) of 1 mg ml^{-1} aggrecan with the mechanical properties of a model solution of 2.5 mg ml^{-1} 1844 kDa HA and 1 mg ml^{-1} aggrecan. (*a*) Average elastic moduli G' for the model solution (average over $n = 17$ beads) and the PCM in the presence (average over $n = 22$ cells) and absence of aggrecan (average over $n = 10$ cells). (*b*) Average viscous moduli G''. Solid line shows the fits by equation (3.2).

Table 1. Mechanical properties of the PCM. Median values of the elastic modulus at the cell surface G'_s and the elastic and viscous characteristic PCM thicknesses λ_E and λ_V, obtained from the G'- and G''-scans, respectively.

	−aggrecan	+aggrecan, −filopodia	+aggrecan, +filopodia	+aggrecan, +HAase
λ_E (μm) (G')	1	3.5	6.5	0
λ_V (μm) (G'')	0.75	4	6.5	0.25
G'_s (Pa)	0.38	0.38	0.43	0.11

reflect the relaxation of a polymer chain section of a length smaller than a network mesh and should therefore depend linearly on polymer concentration. In other words, the magnitude of G'' can be taken as a direct measure of local polymer concentration. The error in G' mostly stems from the error in the estimation of the trap stiffness k_t. A 10 per cent error in k_t corresponds to an approximately 0.1 Pa error in G'. Close to the cell membrane, the increased hydrodynamic interaction between the probe particles and the cell surface dampens the fluctuations of the probe particles and therefore affects both G' and G'' according to Faxen's law (see §2). In figure 2*c*,*d*, we show both the raw data and data corrected using Faxen's law [33]. A comparison shows that the observed overall increase in viscoelasticity near the cell membrane is predominantly owing to the mechanical properties of the PCM and not merely to the presence of the cell surface. For the intact PCM, both G' and G'' have the largest value at the cell surface and decrease with increasing distance from the membrane. We define as characteristic thickness λ of the PCM the height at which the local mechanical response has decayed to $(G_s - G_\infty)/2 + G_\infty$, with G_s the shear modulus (G' or G'') at the cell surface and G_∞ the shear modulus at a height of 25 μm. At the latter height, we could not find a viscoelastic trace of the PCM in any of the cells we tested. The cell shown in figure 2, which was exposed to aggrecan, had a characteristic thickness λ of about 4 μm extracted from both the G' and G'' profiles. This is close to the median value of the 11 cells probed in the presence of aggrecan (table 1). When cells were not incubated with aggrecan, the thickness of the PCM measured in the same way had a distinctly smaller median value of only approximately 1 μm (table 1 for the distribution, electronic supplementary material, figure S3 for indirect visualization with a particle exclusion assay).

3.2. Aggrecan-induced extended pericellular matrix

It has been shown for several cell types that express HA receptors such as CD44 that the co-administration of aggrecan and high molecular-weight HA (but not HA oligomers) induce extended PCMs [12]. It is likely that the exogeneous HA and aggrecan polymers were incorporated into the PCM in these studies. For the PC3 cells used in this study, solely adding aggrecan was sufficient to trigger a PCM extension. One explanation for this could be an electrostatic swelling as proposed by Lee *et al.* [35]. In their theory, the HA chains tethered densely on a cell membrane get extended because of the electrostatic repulsion of the highly charged aggrecan proteoglycans bound to the HA polymers [36]. The thickness of the extended PCM found here (approx. 4 μm) would correspond to the length of HA chains with a molecular weight of around 1600 kDa [37]. HA synthases are indeed capable of synthesizing HA chains more than

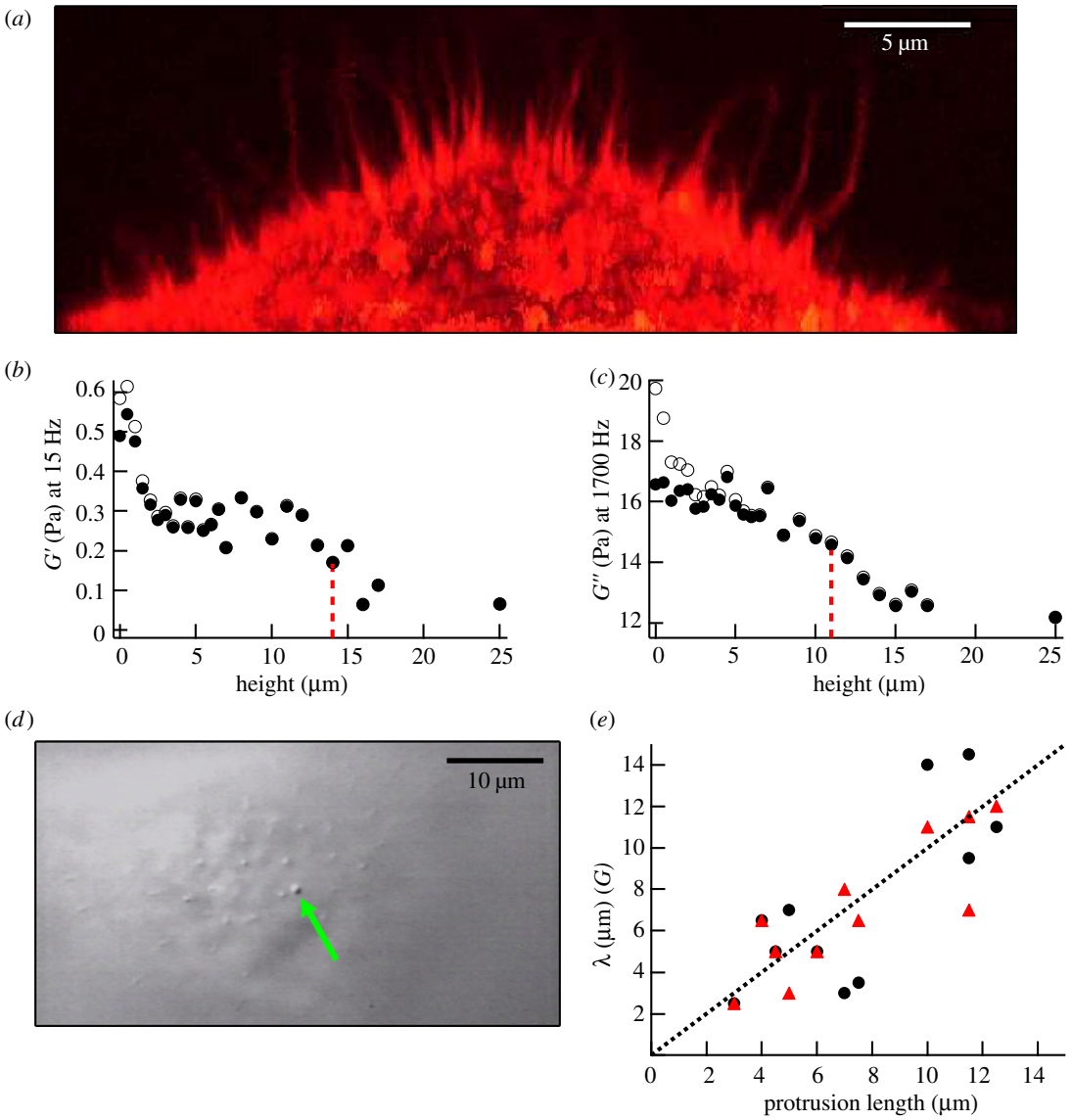

Figure 4. Mechanical properties of the PCM in the spaces between filopodia-like protrusions. (*a*) Long filopodia-like protrusions visualized by staining actin in formaldehyde-fixed cells with Alexa Fluor-555 phalloidin. Vertical projection obtained from a z-stack of horizontal confocal images. (*b*) Vertical cross-section of G' (15 Hz) and (*c*) G'' (1700 Hz) over the pericellular region of the cell imaged in (*d*), expressing straight long protrusions in the presence of aggrecan, corrected (closed circles) and not corrected (open circles) for the hydrodynamic surface effect. (*d*) DIC image with filopodia-like protrusions. The arrow points at a 0.8 µm silica bead trapped in between the protrusions seen in cross section as smaller dots. (*e*) Correlation between PCM thickness λ and length of protrusions. The thickness λ is obtained from G' (circles) or G'' (triangles) height profiles ($n = 11$). The Pearson correlation coefficient of 0.77 (G', closed circles) and 0.85 (G'', closed triangles) indicates a strong correlation between protrusions and PCM. The dotted line shows the equality.

1000 kDa [38]. The tethered HA chains are expected to take a partially collapsed configuration (coil) when they contain a low density of fixed charges (i.e. without aggrecan). Since the Flory radius of a 4 µm long HA chain in good solvent would be approximately 145 nm [37,39], the median thickness of approximately 1 µm for native PCM without exogeneous aggrecan might imply that the HA chains are partly extended because of crowding or to the presence of other endogeneous GAGs.

Instead of the purely physical explanation given by the electrostatic hypothesis, the thickening of the PCM in the presence of aggrecan could be caused by an increased cellular production of PCM components or a decreased shedding of HA from the edge of the PCM. Indeed, a more marked change of cell behaviour together with the further extension of the PCM that we also observed (as shown below) indicates the involvement of cellular signalling processes and an active remodelling of the PCM induced by aggrecan.

3.3. Microrheology in the spaces between filopodia-like protrusions

When PC3 cells were incubated with aggrecan, some cells were found to express several micrometre-long filopodia-like protrusions projecting radially from the cell surface. The protrusions contained actin filaments as shown by confocal fluorescence micrographs of fixed cells stained for actin (figure 4*a*). The protrusions on

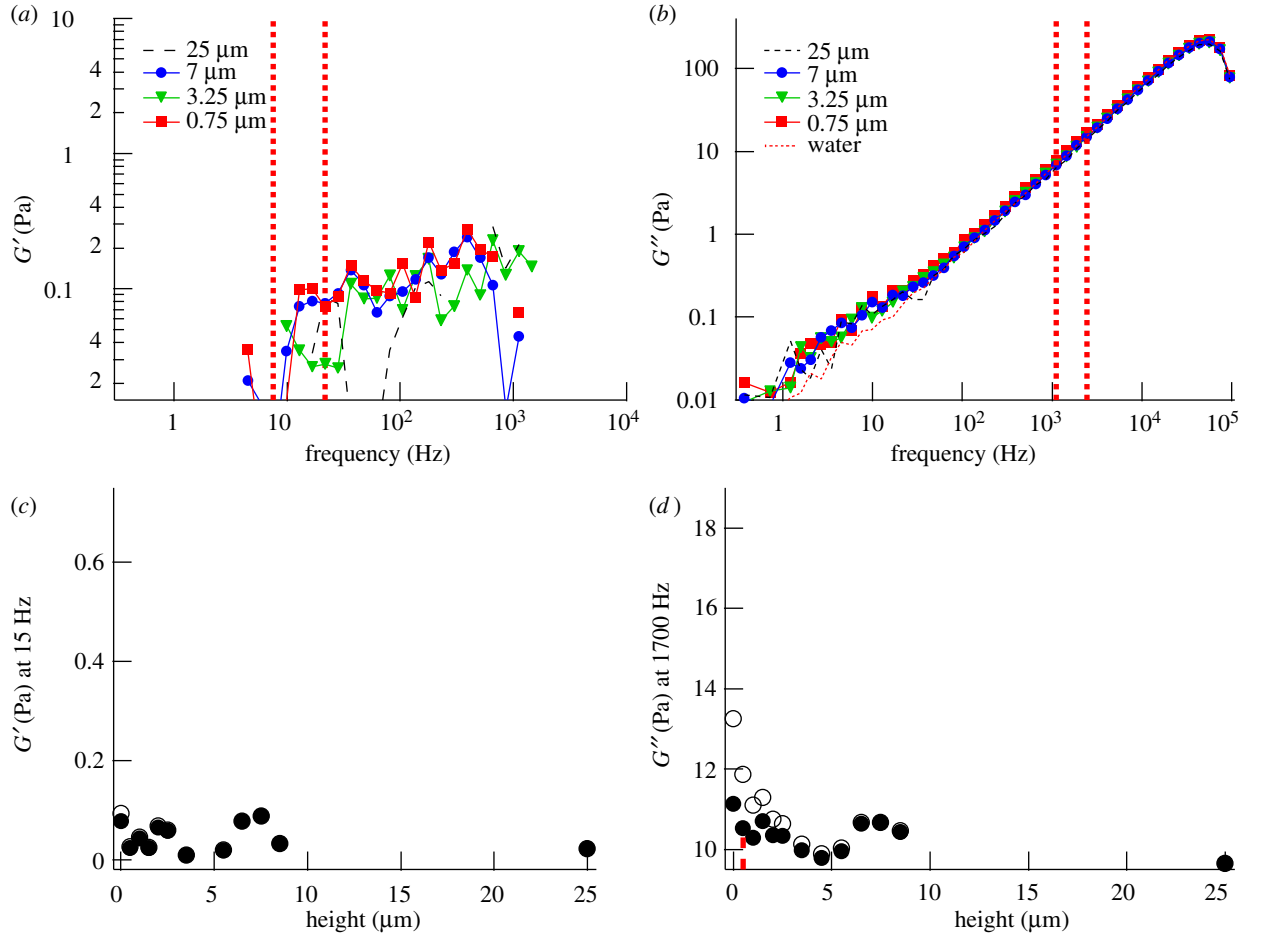

Figure 5. Control experiment after the disruption of the PCM by HAase. (*a*) Elastic and (*b*) viscous moduli at different heights above a PC3 cell incubated with both aggrecan and HAase. (*c*) Radial cross section of G' (15 Hz) and (*d*) G'' (1700 Hz) across the pericellular region in the presence of aggrecan and HAase, corrected (filled circles) and not corrected (open circles) for the hydrodynamic surface effect. Data between vertical dashed lines, 7–22 Hz in (*a*) and 1100–2200 Hz in (*b*), are averaged for each height, and results are shown in (*c*) and (*d*), respectively. Vertical dotted lines indicate the characteristic thickness λ of the PCM.

live cells could also be visualized with high-contrast DIC microscopy during the microrheology experiments (figure 4*d* and electronic supplementary material, movie S1). Protrusion lengths, sometimes more than 10 µm, were measured simultaneously with the microrheology scans. With our scanning microrheology technique, it was possible to probe the viscoelasticity of the PCM in the space between the protrusions. An example of such a scan is shown in figure 4 in which the height dependence of the elastic and viscous moduli is shown. In contrast to what was found with cells not showing protrusions (figure 2), cells expressing protrusions had in some cases a plateau region in the elastic modulus G'. For the example shown in figure 4, G'' remained constant between 2.5 and 15 µm. The characteristic thickness based on the elastic modulus was measured to be $\lambda_E \approx 14$ µm, using $G'_{plateau}$ in the place of G'_s, while the G''-scan gave for the thickness based on the viscous modulus, $\lambda_V \approx 11$ µm. Furthermore, there was a strong correlation between the thickness of the PCM and the length of the protrusions (figure 4*e*). The Pearson correlation coefficient r was 0.77 and 0.85 for the thickness obtained from the G'-scan (circles) and the G''-scan (triangles), respectively. In the presence of the protrusions, the thickness of the PCM was found to be higher with a median value of 6.5 µm (table 1 for the distribution).

In the particle exclusion assay, the PC3 cells showed a round spread-out morphology, which was also seen in a similar experiment reported in the literature [40]. Both the non-treated and aggrecan-treated cells could in our experiments be seen to express filopodia along the substrate (electronic supplementary material, figure S2). Only aggrecan-treated cells, however, were found to express up to about 10 µm long filopodia on top of the cells.

The existence of similar protrusions has been reported for several HA-producing cell types [41] or after transfection of cells with the HA synthase, HAS3 [42]. As these protrusions were found to strongly express HA synthase in their membranes [41], the PCM seems to be, at least partly produced and tethered on the protrusions, and the produced HA might in turn mechanically support the protrusions. Obviously, intracellular stimulation of actin polymerization is necessary to promote the formation of the observed protrusions. Similar phenomena were studied for filopodia formation [43]. Further study will be needed to explore the

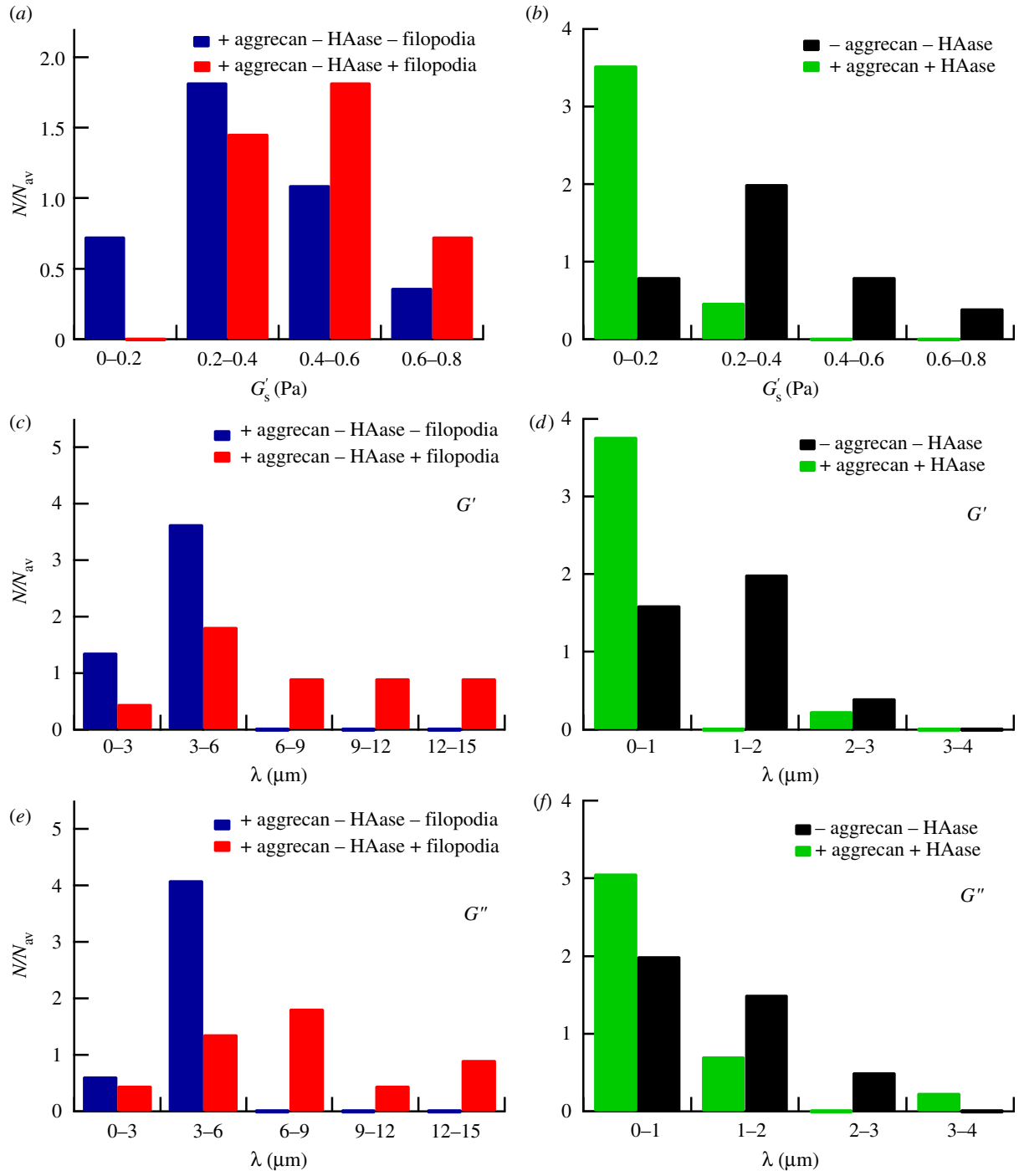

Figure 6. (*a*) Distribution of the elastic moduli at the cell surface G'_s with aggrecan present in the culture medium measured on different cells. A distinction is made between cells showing filopodia-like protrusions (number of different cells, $n = 11$) and cells not showing protrusions ($n = 11$). (*b*) Distribution of G'_s with both aggrecan and HAase ($n = 17$) and without aggrecan and HAase ($n = 10$) present in the culture medium. (*c*,*d*) Distribution of the PCM thickness λ, derived from the G'-scans, measured on different cells (*c*) with aggrecan present in the culture medium without HAase, and (*d*) with, and without both aggrecan and HAase. (*e*,*f*) Same as (*c*,*d*), except values were derived from the G''-scans. N, number of data points per bin; N_{av}, total data points/number of bins.

molecular details causing the thickening of the PCM and the stimulation of protrusions.

3.4. Mechanical consistence and physiological implications of the soft layer

Enzymatic removal of HA disrupted both the soft PCM and the protrusions at any conditions observed. By microrheology, we could not detect a viscoelastic layer any more (figure 5). There remained no visible filopodia-like protrusions. An example of a microrheology scan after HA removal by HAase is shown in figure 5, which shows viscoelastic moduli practically indistinguishable from pure buffer. The increase in viscous modulus near the cell surface was, after this treatment, predominately owing to hydrodynamic interaction

between the probe particle and the cell surface as can be seen in figure 5*d*. We thus conclude that the HA in the PCM rather than aggrecan is the essential factor for the mechanical integrity of the pericellular layer. The absence of an effect of aggrecan on the mechanical properties of the PCM is consistent with the reported experimental observations, where added aggrecan had only moderate effects on HA viscoelasticity [34]. Without HA, no pericellular layer could be found, at least not with our mechanical probes; a median thickness of approximately 0 μm was found (see figure 6*d*,*f* for the distribution and table 1 for the median value).

We measured the PCM of PC3 cells to be relatively soft with a modulus (G'_s) at the cell surface of less than 1 Pa (see figure 6*a*,*b* for the distributions of G'_s and table 1 for the median values for the various conditions (±aggrecan, ±filopodia, ±HAase)). Thus, the PCM of PC3 cells is softer by about a factor 1000 than a typical elastic modulus measured for the cell body [25,44,45]. Such a soft cellular coat will modulate and cushion mechanical interactions between neighbouring cells or between a cell and the ECM and should strongly influence mechanosensory processes that regulate cellular functions in tissues. In the limit of a thin PCM, coupling could be very direct, and numerical modelling suggests that mechanonsensing for example through the clustering of integrins could be mediated by the PCM, and could increase with PCM stiffness [46]. The extreme softness of the PCM of PC3 cells found in our study, in contrast, is in line with the low-adhesion amoeboid motility by which cancer cells can migrate, squeezing through gaps in the ECM [47]. Consistent with such an interpretation, it has been shown that HA is an important factor in cancer cell metastasis; suppression of the HA synthase HAS2, which is responsible for the large HA chains [38], led to a reduced metastasis of breast cancer cells to bone [48]. The same holds for prostate cancer cells, for which it has been shown that the PCM is a requirement for adhesion to bone marrow endothelial cells [40]. Thus, tumour cells may condition their micro-environment with a soft HA-rich PCM to more easily invade surrounding tissues. Furthermore, it was recently reported that HA in the brain ECM plays an important role in the metastatic migration of individual glioma cells [49]: in three-dimensional HA-RGD hydrogels, cells showed non-mesenchymal motility similar to that of glioma cells in brain slice cultures. Cell migration was shown to be dependent on HA concentration, with a complete suppression of invasion at a hydrogel stiffness above 5 kPa.

We here used PC3 prostate cancer cells as a convenient model for a HA-producing cell type, and have studied the effect of the proteoglycan aggrecan on the viscoelastic properties of the PCM of these cells. Aggrecan is not natively incorporated in the PCM of prostate cancer cells, but is usually expressed in the PCM of chondrocytes situated in joint cartilage. Prostate cancer cells, however, have been shown to upregulate the synthesis of versican by fibroblasts in the peritumoral stroma [1]. Aggrecan and versican are similar, belonging to the same hyalectin family, and express the same HA-binding domain, although versican has less CS side chains [7,50]. Furthermore, versican-containing medium, extracted from fibroblast culture, induces thick PCMs similar to those found here [1]. Non-metastatic prostate cancer cells, on the other hand, do not express a PCM [40]. Investigating the viscoelasticity of the PC3–PCM is thus an important step towards exploring the interplay between the mechanics of the PCM and the behaviour of cancer cells.

4. CONCLUSIONS AND OUTLOOK

The high-resolution microrheology technique used in this study is suited for probing the PCM of cells. Using sub-micrometre probe particles, we quantitatively scanned the mechanical properties of the PCM of PC3 prostate cancer cells. One needs to keep in mind, though, that the implicit assumption of a homogeneous medium on the scale of the probe particle is only approximately valid, given the geometrical complexity and inhomogeneity of the cell surface. The maximum elastic modulus of the PCM, which was always found near the cell surface, was less than 1 Pa. This is several orders of magnitude softer than both the elastic modulus of typical cell bodies and extracellular collagen matrices *in vivo*. Addition of exogeneous aggrecan induced striking changes in the PCM; the thickness of the PCM increased together with the emergence of long cellular protrusions. The elastic modulus of the PCM, however, was not significantly affected. As cells are sensitive to mechanical signals from their environment, the mechanical properties of the PCM, which is directly attached and surrounding the cells, are important for cellular functioning. Using microrheology, it will be possible to further explore the biological functions of PCMs of cells in different conditions and, in particular, study the role of these soft layers in cancer cell motility.

This work was supported by the Sonderforschungsbereich SFB 755 of the German Research Foundation (DFG) and by the DFG Center for the Molecular Physiology of the Brain (CMPB). D.M. was further supported by KAKENHI, a programme for the Improvement of the Research Environment for Young Researchers from SCF (Japan).

REFERENCES

1 Ricciardelli, C., Russell, D. L., Ween, M. P., Mayne, K., Suwiwat, S., Byers, S., Marshall, V. R., Tilley, W. D. & Horsfall, D. J. 2007 Formation of hyaluronan- and versican-rich pericellular matrix by prostate cancer cells promotes cell motility. *J. Biol. Chem.* **282**, 10 814–10 825. (doi:10.1074/jbc.M606991200)

2 Guilak, F., Alexopoulos, L. G., Upton, M. L., Youn, I., Choi, J. B., Cao, L., Setton, L. A. & Haider, M. A. 2006 The pericellular matrix as a transducer of biomechanical and biochemical signals in articular cartilage. *Ann. NY Acad. Sci.* **1068**, 498–512. (doi:10.1196/annals.1346.011)

3 Tarbell, J. M., Weinbaum, S. & Kamm, R. D. 2005 Cellular fluid mechanics and mechanotransduction. *Ann. Biomed. Eng.* **33**, 1719–1723. (doi:10.1007/s10439-005-8775-z)

4 Evanko, S. P., Angello, J. C. & Wight, T. N. 1999 Formation of hyaluronan- and versican-rich pericellular matrix is required for proliferation and migration of

vascular smooth muscle cells. *Arterioscler. Thromb. Vasc. Biol.* **19**, 1004–1013. (doi:10.1161/01.ATV.19.4.1004)
5 van den Berg, B. M., Vink, H. & Spaan, J. A. 2003 The endothelial glycocalyx protects against myocardial edema. *Circ. Res.* **92**, 592–594. (doi:10.1161/01.RES.0000065917.53950.75)
6 Henry, C. B. & Duling, B. R. 1999 Permeation of the luminal capillary glycocalyx is determined by hyaluronan. *Am. J. Physiol.* **277**, H508–H514.
7 Mochizuki, S., Vink, H., Hiramatsu, O., Kajita, T., Shigeto, F., Spaan, J. A. & Kajiya, F. 2003 Role of hyaluronic acid glycosaminoglycans in shear-induced endothelium-derived nitric oxide release. *Am. J. Physiol. Heart Circ. Physiol.* **285**, H722–H726. (doi:10.1152/ajpheart.00691.2002)
8 Pries, A. R., Secomb, T. W. & Gaehtgens, P. 2000 The endothelial surface layer. *Pflugers Arch.* **440**, 653–666. (doi:10.1007/s004240000307)
9 Hosono, K., Nishida, Y., Knudson, W., Knudson, C. B., Naruse, T., Suzuki, Y. & Ishiguro, N. 2007 Hyaluronan oligosaccharides inhibit tumorigenicity of osteosarcoma cell lines MG-63 and LM-8 *in vitro* and *in vivo* via perturbation of hyaluronan-rich pericellular matrix of the cells. *Am. J. Pathol.* **171**, 274–286. (doi:10.2353/ajpath.2007.060828)
10 Kiani, C., Chen, L., Wu, Y. J., Yee, A. J. & Yang, B. B. 2002 Structure and function of aggrecan. *Cell Res.* **12**, 19–32. (doi:10.1038/sj.cr.7290106)
11 Wight, T. N. 2002 Versican: a versatile extracellular matrix proteoglycan in cell biology. *Curr. Opin. Cell Biol.* **14**, 617–623. (doi:10.1016/S0955-0674(02)00375-7)
12 Knudson, W. & Knudson, C. B. 1991 Assembly of a chondrocyte-like pericellular matrix on non-chondrogenic cells. Role of the cell surface hyaluronan receptors in the assembly of a pericellular matrix. *J. Cell Sci.* **99**(Pt 2), 227–235.
13 Solon, J., Levental, I., Sengupta, K., Georges, P. C. & Janmey, P. A. 2007 Fibroblast adaptation and stiffness matching to soft elastic substrates. *Biophys. J.* **93**, 4453–4461. (doi:10.1529/biophysj.106.101386)
14 Hadjipanayi, E., Mudera, V. & Brown, R. A. 2009 Close dependence of fibroblast proliferation on collagen scaffold matrix stiffness. *J. Tissue Eng. Regen. Med.* **3**, 77–84. (doi:10.1002/term.136)
15 Kostic, A., Lynch, C. D. & Sheetz, M. P. 2009 Differential matrix rigidity response in breast cancer cell lines correlates with the tissue tropism. *PLoS ONE* **4**, e6361. (doi:10.1371/journal.pone.0006361)
16 Engler, A. J., Sen, S., Sweeney, H. L. & Discher, D. E. 2006 Matrix elasticity directs stem cell lineage specification. *Cell* **126**, 677–689. (doi:10.1016/j.cell.2006.06.044)
17 Lam, W. A., Cao, L., Umesh, V., Keung, A. J., Sen, S. & Kumar, S. 2010 Extracellular matrix rigidity modulates neuroblastoma cell differentiation and N-myc expression. *Mol. Cancer* **9**, 35. (doi:10.1186/1476-4598-9-35)
18 Alexopoulos, L. G., Williams, G. M., Upton, M. L., Setton, L. A. & Guilak, F. 2005 Osteoarthritic changes in the biphasic mechanical properties of the chondrocyte pericellular matrix in articular cartilage. *J. Biomech.* **38**, 509–517. (doi:10.1016/j.jbiomech.2004.04.012)
19 Darling, E. M., Wilusz, R. E., Bolognesi, M. P., Zauscher, S. & Guilak, F. 2010 Spatial mapping of the biomechanical properties of the pericellular matrix of articular cartilage measured in situ via atomic force microscopy. *Biophys J* **98**, 2848–2856. (doi:10.1016/j.bpj.2010.03.037)
20 MacKintosh, F. C. & Schmidt, C. F. 1999 Microrheology. *Curr. Opin. Colloid Interf. Sci.* **4**, 300–307. (doi:10.1016/S1359-0294(99)90010-9)
21 Ricciardelli, C., Mayne, K., Sykes, P. J., Raymond, W. A., McCaul, K., Marshall, V. R. & Horsfall, D. J. 1998 Elevated levels of versican but not decorin predict disease progression in early-stage prostate cancer. *Clin. Cancer Res.* **4**, 963–971.
22 Lipponen, P., Aaltomaa, S., Tammi, R., Tammi, M., Agren, U. & Kosma, V. M. 2001 High stromal hyaluronan level is associated with poor differentiation and metastasis in prostate cancer. *Eur. J. Cancer* **37**, 849–856. (doi:S0959804900004482)
23 Gittes, F., Schnurr, B., Olmsted, P. D., MacKintosh, F. C. & Schmidt, C. F. 1997 Microscopic viscoelasticity: shear moduli of soft materials determined from thermal fluctuations. *Phys. Rev. Lett.* **79**, 3286–3289. (doi:10.1103/PhysRevLett.79.3286)
24 Allersma, M. W., Gittes, F., deCastro, M. J., Stewart, R. J. & Schmidt, C. F. 1998 Two-dimensional tracking of ncd motility by back focal plane interferometry. *Biophys. J.* **74**, 1074–1085. (doi:10.1016/S0006-3495(98)74031-7)
25 Bacabac, R. G., Mizuno, D., Schmidt, C. F., MacKintosh, F. C., Van Loon, J. J., Klein-Nulend, J. & Smit, T. H. 2008 Round versus flat: bone cell morphology, elasticity, and mechanosensing. *J. Biomech.* **41**, 1590–1598. (doi:10.1016/j.jbiomech.2008.01.031)
26 Atakhorrami, M., Sulkowska, J. I., Addas, K. M., Koenderink, G. H., Tang, J. X., Levine, A. J., Mackintosh, F. C. & Schmidt, C. F. 2006 Correlated fluctuations of microparticles in viscoelastic solutions: quantitative measurement of material properties by microrheology in the presence of optical traps. *Phys. Rev. E* **73**, 061 501. (doi:10.1103/PhysRevE.73.061501)
27 Atakhorrami, M. & Schmidt, C. F. 2006 High-bandwidth one- and two-particle microrheology in solutions of wormlike micelles. *Rheol. Acta* **45**, 449–456. (doi:10.1007/s00397-005-0071-1)
28 Peterman, E. J., Gittes, F. & Schmidt, C. F. 2003 Laser-induced heating in optical traps. *Biophys. J.* **84**, 1308–1316. (doi:10.1016/S0006-3495(03)74946-7)
29 Buchanan, M., Atakhorrami, M., Palierne, J. F., MacKintosh, F. C. & Schmidt, C. F. 2005 High-frequency microrheology of wormlike micelles. *Phys. Rev. E* **72**, 011504. (doi:10.1103/PhysRevE.72.011504)
30 Addas, K. M., Schmidt, C. F. & Tang, J. X. 2004 Microrheology of solutions of semiflexible biopolymer filaments using laser tweezers interferometry. *Phys. Rev. E* **70**, 021 503. (doi:10.1103/PhysRevE.70.021503)
31 Nijenhuis, N., Mizuno, D., Schmidt, C. F., Vink, H. & Spaan, J. A. 2008 Microrheology of hyaluronan solutions: implications for the endothelial glycocalyx. *Biomacromolecules* **9**, 2390–2398. (doi:10.1021/bm800381z)
32 Vermeulen, K. C., Wuite, G. J., Stienen, G. J. & Schmidt, C. F. 2006 Optical trap stiffness in the presence and absence of spherical aberrations. *Appl. Opt.* **45**, 1812–1819. (doi:10.1364/AO.45.001812)
33 Faxen, H. 1923 Die Bewegung einer Starren Kugel längs der Achse eines mit zäher Flüssigkeit gefüllten Rohres. *Ark. Mat. Astron. Fys.* **17**, 1–28.
34 Nijenhuis, N., Mizuno, D., Spaan, J. A. & Schmidt, C. F. 2009 Viscoelastic response of a model endothelial glycocalyx. *Phys. Biol.* **6**, 025014. (doi:10.1088/1478-3975/6/2/025014)
35 Lee, G. M., Johnstone, B., Jacobson, K. & Caterson, B. 1993 The dynamic structure of the pericellular matrix on living cells. *J. Cell Biol.* **123**, 1899–1907. (doi:10.1083/jcb.123.6.1899)
36 Hellmann, M., Weiss, M. & Heermann, D. W. 2007 Monte Carlo simulations reveal the straightening of an end-grafted flexible chain with a rigid side chain. *Phys. Rev. E* **76**, 021 802. (doi:10.1103/PhysRevE.76.021802)

37 Atkins, E. D., Phelps, C. F. & Sheehan, J. K. 1972 The conformation of the mucopolysaccharides. Hyaluronates. *Biochem. J.* **128**, 1255–1263.
38 Itano, N. *et al.* 1999 Three isoforms of mammalian hyaluronan synthases have distinct enzymatic properties. *J. Biol. Chem.* **274**, 25 085–25 092. (doi:10.1074/jbc.274.35.25085)
39 Degennes, P. G. 1987 Polymers at an interface: a simplified view. *Adv. Colloid Interface Sci.* **27**, 189–209. (doi:10.1016/0001-8686(87)85003-0)
40 Simpson, M. A., Reiland, J., Burger, S. R., Furcht, L. T., Spicer, A. P., Oegema Jr, T. R. & McCarthy, J. B. 2001 Hyaluronan synthase elevation in metastatic prostate carcinoma cells correlates with hyaluronan surface retention, a prerequisite for rapid adhesion to bone marrow endothelial cells. *J Biol Chem* **276**, 17 949–17 957. (doi:10.1074/jbc.M010064200M010064200)
41 Rilla, K., Tiihonen, R., Kultti, A., Tammi, M. & Tammi, R. 2008 Pericellular hyaluronan coat visualized in live cells with a fluorescent probe is scaffolded by plasma membrane protrusions. *J. Histochem. Cytochem.* **56**, 901–910. (doi:10.1369/jhc.2008.951665)
42 Kultti, A., Rilla, K., Tiihonen, R., Spicer, A. P., Tammi, R. H. & Tammi, M. I. 2006 Hyaluronan synthesis induces microvillus-like cell surface protrusions. *J. Biol. Chem.* **281**, 15 821–15 828. (doi:10.1074/jbc.M512840200)
43 Yang, C., Czech, L., Gerboth, S., Kojima, S., Scita, G. & Svitkina, T. 2007 Novel roles of formin mDia2 in lamellipodia and filopodia formation in motile cells. *PLoS Biol.* **5**, e317. (doi:10.1371/journal.pbio.0050317)
44 Mahaffy, R. E., Park, S., Gerde, E., Kas, J. & Shih, C. K. 2004 Quantitative analysis of the viscoelastic properties of thin regions of fibroblasts using atomic force microscopy. *Biophys. J.* **86**, 1777–1793. (doi:10.1016/S0006-3495(04)74245-9)
45 Wu, H. W., Kuhn, T. & Moy, V. T. 1998 Mechanical properties of L929 cells measured by atomic force microscopy: effects of anticytoskeletal drugs and membrane crosslinking. *Scanning* **20**, 389–397. (doi:10.1002/sca.1998.4950200504)
46 Paszek, M. J., Boettiger, D., Weaver, V. M. & Hammer, D. A. 2009 Integrin clustering is driven by mechanical resistance from the glycocalyx and the substrate. *PLoS Comput. Biol.* **5**, e1000604. (doi:10.1371/journal.pcbi.1000604)
47 Sahai, E. 2005 Mechanisms of cancer cell invasion. *Curr. Opin. Genet. Dev.* **15**, 87–96. (doi:10.1016/j.gde.2004.12.002)
48 Urakawa, H., Nishida, Y., Wasa, J., Arai, E., Zhuo, L., Kimata, K., Kozawa, E., Futamura, N. & Ishiguro, N. 2011 Inhibition of hyaluronan synthesis in breast cancer cells by 4-methylumbelliferone suppresses tumorigenicity *in vitro* and metastatic lesions of bone *in vivo*. *Int. J. Cancer* **130**, 454–456. (doi:10.1002/ijc.26014)
49 Ananthanarayanan, B., Kim, Y. & Kumar, S. 2011 Elucidating the mechanobiology of malignant brain tumors using a brain matrix-mimetic hyaluronic acid hydrogel platform. *Biomaterials* **32**, 7913–7923. (doi10.1016/J.Biomaterials.2011.07.005)
50 Dours-Zimmermann, M. T. & Zimmermann, D. R. 1994 A novel glycosaminoglycan attachment domain identified in two alternative splice variants of human versican. *J. Biol. Chem.* **269**, 32 992–32 998.